SCIENTIFIC REPORTS

OPEN

Destruction of Tissue, Cells and Organelles in Type 1 Diabetic Rats Presented at Macromolecular Resolution

Raimond B. G. Ravelli[1], Ruby D. Kalicharan[2], M. Cristina Avramut[1], Klaas A. Sjollema[2], Joachim W. Pronk[1], Freark Dijk[2], Abraham J. Koster[1], Jeroen T. J. Visser[2], Frank G. A. Faas[1] & Ben N. G. Giepmans[2]

[1]Dept. Molecular Cell Biology, Leiden University Medical Center, P. O. Box 9600, 2300 RC, Leiden, The Netherlands, [2]Dept. of Cell Biology, University Medical Center Groningen, University of Groningen, P. O. Box 196, 9700 AD, Groningen, The Netherlands.

Finding alternatives for insulin therapy and making advances in etiology of type 1 diabetes benefits from a full structural and functional insight into Islets of Langerhans. Electron microscopy (EM) can visualize Islet morphology at the highest possible resolution, however, conventional EM only provides biased snapshots and lacks context. We developed and employed large scale EM and compiled a resource of complete cross sections of rat Islets during immuno-destruction to provide unbiased structural insight of thousands of cells at macromolecular resolution. The resource includes six datasets, totalling 25.000 micrographs, annotated for cellular and ultrastructural changes during autoimmune diabetes. Granulocytes are attracted to the endocrine tissue, followed by extravasation of a pleiotrophy of leukocytes. Subcellullar changes in beta cells include endoplasmic reticulum stress, insulin degranulation and glycogen accumulation. Rare findings include erythrocyte extravasation and nuclear actin-like fibers. While we focus on a rat model of autoimmune diabetes, our approach is general applicable.

Diabetes Mellitus is a life-threatening disease, and its incidence continues to increase, now affecting over 8% of mankind[1]. The two most prevailing forms are type 2 diabetes, which is caused by insulin-resistance combined with a relative deficiency in insulin, and type 1 diabetes. In the latter, insulin-producing beta cells are destroyed by an autoimmune attack. Upon diagnosis, life-long exogenous insulin therapy is immediately initiated[2]. Fundamental questions in type 1 diabetes remain: What are the triggers? Can it be prevented? Can we diagnose and immune suppress at-onset or near-onset diabetes? Can patients be cured? To address these questions, microscopy is often pivotal, for example to analyze transplanted Islets[3,4], or to assess the success of creating insulin-producing cells[5]. Soon after Gray published the macroscopic anatomy of the pancreas[6], a seminal microscopic observation was made by Langerhans[7]: *"cells are small and have an irregular polygonal formation with a completely homogenous content, gleamy and free from granules. Their nucleus is bright, round and middle-sized. The cells are 0.0096 to 0.012 mm, the nuclei 0.0075 to 0.008 mm in diameter. Mostly, several cells are in close proximity, distributed peculiarly in the Parenchym of the gland"*. These clustered cells are now known as Islets of Langerhans (Islets), consisting primarily of beta cells that are destroyed in type 1 diabetes[8]. Although Langerhans' description was accurate, sharing microscopic images is invaluable. Unfortunately, electron microscopists need to make stringent subjective selections prior to publishing high-resolution snapshots of a small field of view. We developed[9] and implemented large-scale EM to visualize the nano-anatomy (nanotomy) of Islets at different stages of diabetes. The data are presented in a way that allows unbiased analysis by a broad (scientific) community.

Results

The nanotomy technique. A prerequisite for nanotomy is complete sampling of tissues, preventing that samples become obscured during preparation (Fig. 1a). Since Islets constitute only ~1% of the pancreas, light microscopy is needed to guide Islets section preparation on special carriers (Fig. 1a–e). Following EM quality control, automated EM-acquisition and stitching is applied (See Methods). Nanotomy thus generates large-scale (Fig. 1f) high-resolution maps allowing inspection of macromolecules anywhere in the dataset (Fig. 1g–k).

An overview of tissue, cells, organelles and macromolecules. Six datasets at different stages of diabetes progression are presented (Fig. 2). Several features have been annotated and selected cells have been false colored to
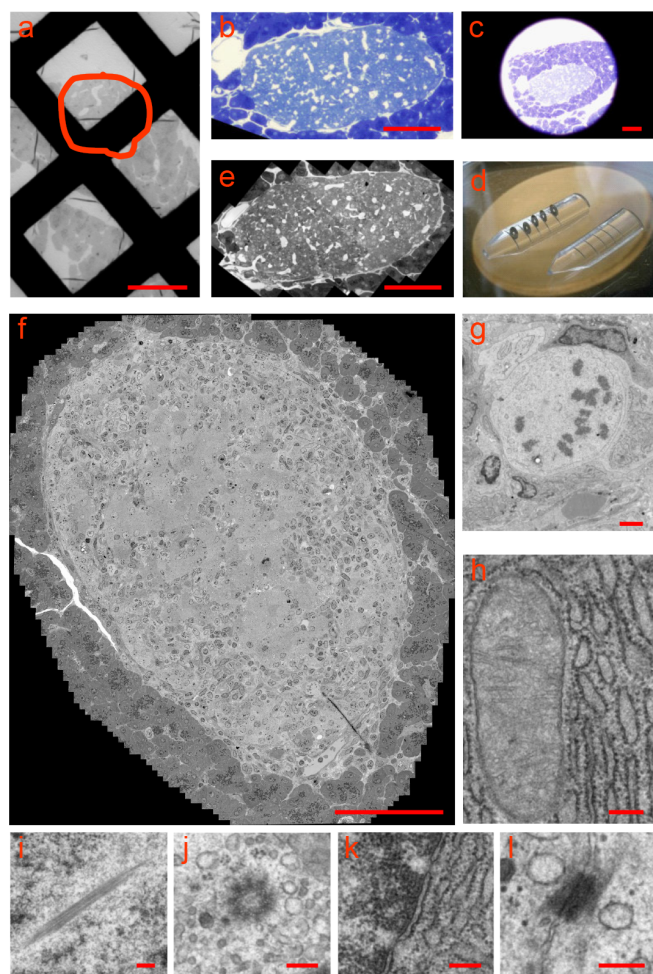
Figure 1 | EM of a single Islet in situ: Procedure. Clockwise: (a) Classical grids for EM cannot be used since grid bars (black) significantly overlap with the Islet (outlined in red; ~0.2 mm × 0.2 mm; bar 0.1 mm). (b) 1 μm Epon semi-thin pancreas section (normal Wistar rat) stained with toluidine blue: the Islet (~0.7 × 0.3 mm) colors light blue (bar 0.1 mm). (c) Positioning of the 1 μm semi-thin section on a single-hole nickel grid (hole is 1 mm in diameter) prior to thin sectioning (bar 0.5 mm). (d) Single hole grids prepared with stabilizing formvar film and ultrathin sections (60 nm) in position for staining. (e) Composition of 21 manually collected EM images using traditional analog acquisition on film and manual stitching of the complete Islet. (f; online: V-1F) Nanotomy following automated acquisition and stitching allows to analyze any area at high resolution, for instance to analyze (g; V-10A) mitotic cells; (h; V-3A) mitochondria (left) and rough ER (right); (i; V-10F) nuclear actin-like structures; (j; V-7J) centriole; (k; V-7A) nuclear pores; (l; V-7E) desmosomes. Bars: 100 μm (a–e); 500 μm (f); 1 μm (g); 100 nm (h–l).

indicate different cell types, such as insulin-producing beta cells (green) and glucagon-producing alpha cells (yellow). Figure 2 shows a low-magnification summary of the data: the full extent of our nanotomy data can only be appreciated online (www.nanotomy.nl). Prior to focusing on the effect of type 1 diabetes, an online tour on ultrastructure interpretation is given for the reader less experienced with EM-analysis, starting with dataset I (diabetic resistant); group 2 (cell types); letter A (acinar cell), or I-2A in short. Acinar cells are part of the exocrine pancreas surrounding the Islet, which also contains the characteristic duct cells (I-2E). The endocrine pancreas contains alpha cells (I-2B), beta cells (I-2C), PP1 (see below) and delta cells (I-2D), as well as multiple capillaries harboring erythrocytes (I-2G) and leukocytes (I-2F). Our

large-scale approach significantly increases the chances to observe less-abundant cells, such as eosinophil granulocytes (IV-2I) and basophil granulocytes (IV-2J). Nanotomy allows for sub-cellular analysis of organelles, granules and supramacromolecules, which are indicative for cell identity and function. Nuclei, for instance, are absent in erythrocytes (V-2H), occupy most of the volume in lymphocytes (V-2G) and are horseshoe-like in monocytes (V-2I). Mitotic cells are distinguished by the absence of a nucleus (V-10A) and the condensation of chromatin (V-10E). A shrunk structure-less nucleus is characteristic for pyknotic cells (IV-2H). The Golgi apparatus (V-3D) and rough endoplasmic reticulum (ER; V-3A) are abundant in the secretory cells. Zooming in and out aids to identify the substance of secretory granules: zymogen (V-4A), insulin (V-4B), glucagon (V-4F), somatostatin (V-4G) and pancreatic polypeptide (PP). Several macromolecular complexes can be identified, such as nuclear pores (V-7A side view; V-7B top view; Fig. 1k); polysomes (V-7C); ribosomes (V-7D) and cell-cell junctions, including gap junctions, tight junctions (V-7F) and desmosomes (V-7E; Fig. 1l). Rare macromolecular structures include fibers in a nucleus (V-10F; Fig. 1l), possibly the debated filamentous nuclear actin[10]. Curled membranes within insulin granules are seen (V-4E), which will likely become exosomes upon insulin secretion. These datasets provide a detailed and interactive view of cellular ultrastructure in Islets of Langerhans.

Islets under attack. To analyze the onset and progression of diabetes with nanotomy, we analyzed Islets in diabetes-prone (DP) Bio Breeding (BB) rats, in which blood glucose (BG) levels are indicative of the (pre)diabetic state. The DP animals are lymphopenic: the shortage of regulatory T cells leads to a spontaneous autoimmune attack of the beta cells in most animals with approximately half of the population affected around 80 days[11]. In control diabetes resistant (DR) BB rats, beta cells look normal with abundant presence of insulin granules and normal nuclei (I-2C). Signs of leukocytes extravasating the endocrine or exocrine capillaries are absent, though leukocytes are found inside the vasculature (I-2F). The Islet of the DP rat with the lowest BG tested (7.2 mM; II) shows morphological characteristic comparable to the control. Numerous apoptotic beta cells are observed in the 9.9 mM data set (III): these cells contain abundant insulin but have characteristic swollen vesicles, dark cytoplasm and condensed chromatin (III-2H). At this stage, no sign of insulitis[12] is present, but an apparent increased leukocyte to erythrocyte ratio in the vasculature compared to DR rats hints at an immune activation. At the periphery of the Islet extravasated leukocytes are present. The Islet of the rat with 12 mM BG (IV) shows extensive insulitis and morphological changes. Healthy beta cells with abundant insulin content as well as exhausted beta cells with empty granules are present. More beta cells are being phagocytosed at this stage of diabetes. In a more advanced stage (23 mM; V), massive endocrine extravasation is present: the Islet is filled with a pleiotrophy of leukocytes. Most beta cells show compromised morphology and are being attacked (V-9A,B), phagocytosed and digested (V-9C to G). Lastly, we show a cross-section of an Islet at the end stage of type 1 diabetes (VI). The majority of this section consists of alpha cells (VI-2B), while only some leukocytes are present (VI-2E). Intact beta cells are no longer detectable within this dataset. Our observations expand on earlier reports of insulitis using mainly light microscopic techniques[13–17]. First apoptotic cells are present in the pre-diabetic state. At a later stage, a pleiotrophy of leukocytes extravasate, resulting in massive insulitis, possibly attracted by chemokines and macrophage activation. In our rat model, leukocyte extravasation seems to originate directly from the endocrine tissue. Intravital imaging of insulitis induced by viral infection in mice[18] showed exocrine leukocyte extravasation followed by random walk migration. The distinct mode of insulitis might differ between species or
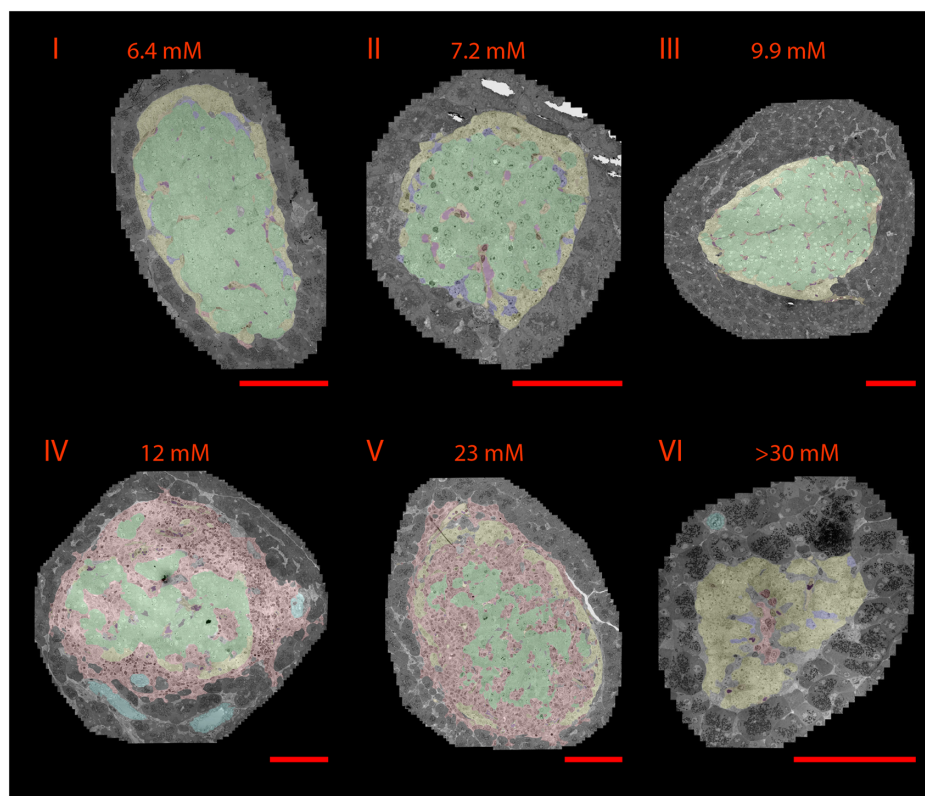
Figure 2 | Analysis of Islets of Langerhans during autoimmune diabetes progression. Automated acquisition and stitching of an entire Islet section allows analysis at different levels of magnification. Individual cells were morphologically characterized and false-colored according to cell-type (outlined in Methods): green (beta cells), yellow (alpha cells), red (leukocytes), purple (ducts) and cyan (vasculature). (I) Diabetes resistant rat; (II)–(VI) diabetes prone rat at different stages of (pre)diabetes, as indicated by the blood sugar (BG) levels. Note the massive infiltration of leukocytes (red) and destruction of beta cells (green). Bars: 0.1 mm. For full resolution, visit www.nanotomy.nl.
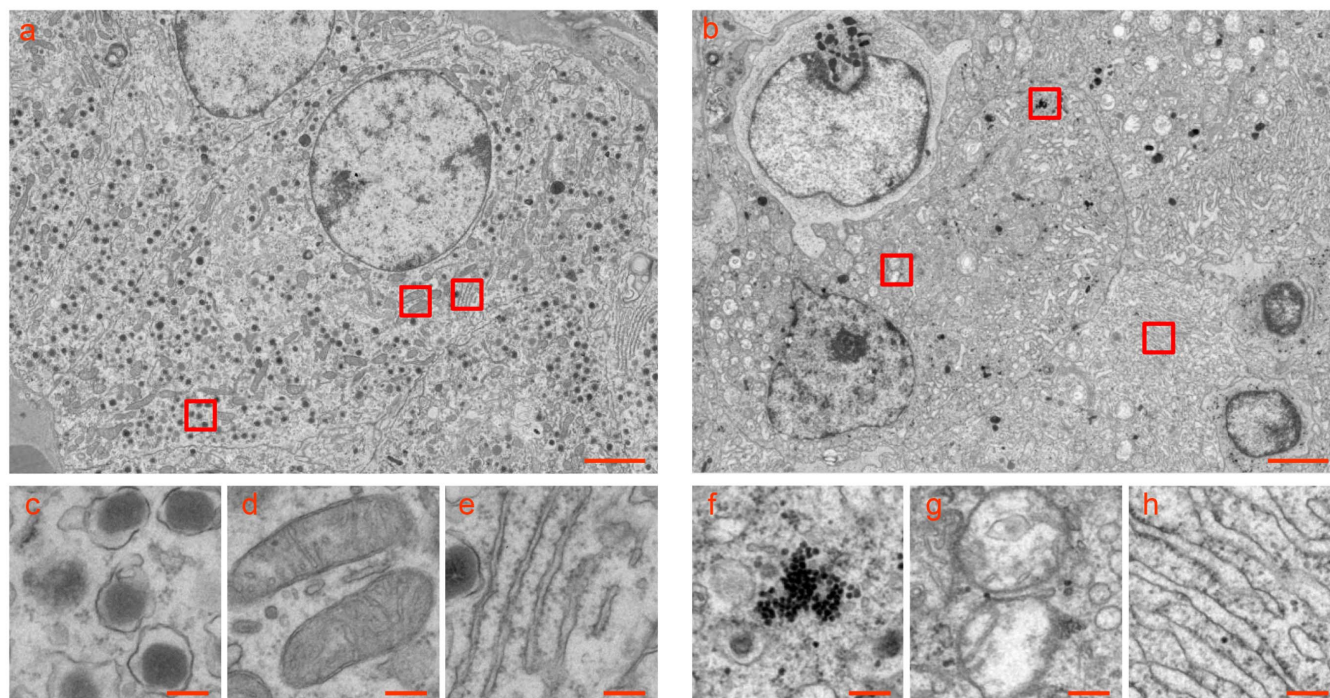

Figure 3 | Subcellular hallmarks of of beta cell destruction during diabetes. Two areas of the EM-datasets of a healthy (a; BG 6.4 mM; I-3C) and diabetic (b; BG 23 mM; V-10G) animal are shown. The boxed areas show close-ups of normal insulin-containing granules (c; I-3D), normal mitochondria (d; I-3E), and normal ER (e; I-3F) for the healthy animal. The diabetic animal shows accumulation of electron-dense glycogen particles (f; V-10H), mitochondrial destruction (g; V-10I) and ER-dilation (h; V-10J). Bars: 1 μm (a,b); 100 nm (c–h). For full resolution, visit www.nanotomy.nl.

animal model. At the late stage of Islet destruction, leukocytes are no longer needed and most have left the Islet.

Subcellular changes during type 1 diabetes. Besides cellular information, nanotomy allows analyzing macromolecular and organelle features throughout the datasets. The endocrine tissue has a dense network of micro-vasculature, which is surrounded by a basement membrane. In the diabetic animals, several extravasated leukocytes seem to be surrounded by an additional basement membrane, particular when they are in the vicinity of the vasculature (V-6E). In humans, a double basement membrane is present around the Islets[19]. Our results suggest that this is also the case in rats: leukocytes are temporarily caught within these two basement membranes during extravasation. Interestingly, multi-layered vascular basement membranes have also been observed in the context of other diseases[20].

The endoplasmic reticulum (ER) in beta cells (Fig. 3; V-10J) of the diabetic Islets becomes perturbed: their dilation is a sign of ER stress. The ultrastructure of mitochondria is also affected. Cisternae are clearly distinguishable in normal mitochondria (Fig. 3d; I-3E), whereas mitochondria are rearranged in beta cells of the diabetic Islets (Fig. 3g; V-10I) and, in a final stage, become hard to recognize. Fig. 3 shows a comparison of a healthy versus a high BG beta cell. Note that the insulin granules are hardly present in the latter (V-10G): the large demand for insulin for the high BG animal exhausted these granules.

Particles accumulate in beta cells during diabetes progression. Another striking feature in beta cells of diabetic animals is the accumulation of clusters of darkly stained particles, measuring ~35 nm in size (Fig. 3f; V-10H), and often associated with membranes (Fig. 4a; V-10B). For the non-diabetic animals, these particles are found associated with the vasculature (I-3A) and ducts (I-3B), whereas for the diabetic animals isolated spots are found in leukocytes (V-10D) and clustered spots with the beta cells (Fig. 3f; V-10B;). Only at the final stage of diabetes, when most beta cells are destroyed, the particles are also seen in other endocrine cells. Viruses, in particular enteroviruses, have been named as potential triggers for type 1 diabetes[12,21], and in man similar particles were presented as viruses[21]. BB rats were found to be infected with Ljungan virus[22], however, our anti-Ljungan virus immunolabeling experiments on these particles were either negative or non-conclusive (data not shown). 3D reconstruction of one of the particle-membrane clusters (Fig. 4b) shows that these particles vary in size and do not appear polyhedral, arguing against the possibility that these may be viruses. Presence of glycogen in beta cells, apparent as particles of 10–30 nm, has been linked to diabetes previously[23,24]. The degree of glycogenic infiltration varies from one beta cell to the next and an inverse relationship between the degree of granulation and the extent of glycogen deposition has been reported[25]. The particles in our samples must be glycogen as concluded from positive silver staining against polysaccharides (Fig. 4). Additional physiological studies are needed to address whether glycogen accumulation, a probable consequence of elevated blood glucose levels, plays a role in diabetes development.

Discussion

Nanotomy provides a wealth of ultrastructural information online and can be applied to all kinds of tissues and diseases. Our analysis of Islets of Langerhans during autoimmune diabetes onset in a rat model reveals, among others, glycogen particles associated with diabetes progression. Other rare features are mitotic cells (V-10A), nuclear fibers that resemble actin (V-10F) and an extravasated erythrocyte (II-3A); many more unique events wait to be discovered, highlighted and interpreted within nanotomy data, aided by open access analysis. Viruses, implicated in triggering type 1 diabetes in man[21], present within Islets should be detectable by our technique.

The fact that we could not detect viruses argues against the debated endemic presence of Ljungan picornavirus in BB rats[26]. While the datasets contain information on thousands of cells and a multifold thereof of macromolecules, we note that presently only a single cross-section of each Islet is shown. The typical and rare events observed in the datasets should become significant by generic implementation and expansion of nanotomy, including human Islets that have a very distinct organization than rodent Islets. Moreover, large-scale EM-imaging, possibly combined with 3D approaches[27,28] will allow assessing effects of gene-mutations in genetically-modified organisms, within the cellular context at a molecular scale. Annotation might not only be performed by morphological examination, but also by labeling, including correlated microscopy[29]. Both scientists as well as the public (patients) can interactively access our data to address what goes wrong with Islets, cells, organelles and macromolecules during type 1 diabetes onset in this rat model, which will be followed up in
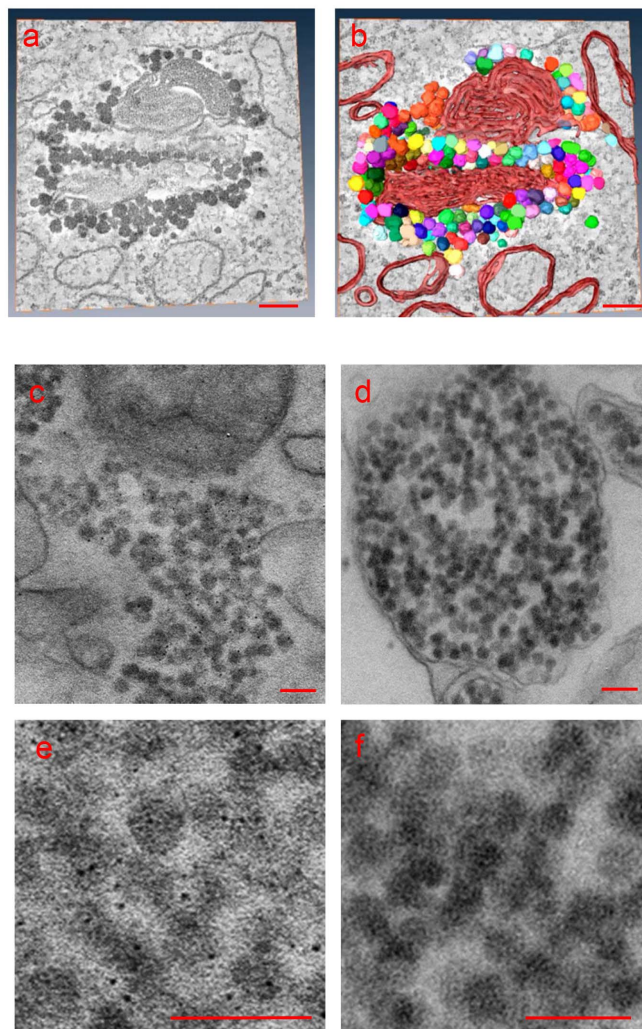

Figure 4 | Glycogen accumulation in beta cells during autoimmune diabetes onset. (a,b) A 3D double-tilt tomographic reconstruction analysis from a thin section shows a close association of glycogen particles (~35 nm in diameter) with membranes (in orange). (a) shows a slice through the tomogram, (b) a segmentation of the volume made with *Amira* (Visage Imaging). The particles lack systematic polyhedral appearance and differ in size. (c–f) Polysaccharide staining using the Thiery method (see Methods) reveals a fine speckled silver deposition on the particles, indicating that these are polysaccharide-rich. This fine precipitate is not present in the negative control, where periodic acid treatment has been omitted from the reaction[33]. Bars: 100 nm.

Table 1 | Data set statistics and rat parameters

Nr	DP/DR	BG (mM)	Sex	Age (days)	Voltage (kV)	Images (n)	Acq. time (min; hr)	Size x*y (μm)	Size (Gpixel)
I	DR	6.4	f	76	80	2352	258; 4.3	247 × 341	8.4
II	DP	7.2	f	74	80	1855	224; 3.7	234 × 274	6.4
III	DP	9.9	m	70	80	6879	831; 14	490 × 468	23
IV	DP	12	m	76	120	6876	896; 15	507 × 471	24
V	DP	23	m	68	120	5908	741; 12	414 × 476	20
VI	DP	>30	f	83	120	1564	235; 3.9	211 × 224	4.7

Nr: Number dataset. DP/DR: Diabetes prone/Diabetes resistant. Acq. Time: Microscope data acquisition time. Gpixel: gigapixel.

human Islets of Langerhans and may aid in uncovering the trigger(s) and help developing new therapies.

Methods

Animals. The rats were derived from the Worcester DP-BB and DR-BB strain, and were maintained and bred at our institutional Central Animal Facility[30,31]. The animals received humane care in compliance with the principles of laboratory animal care (NIH publication no. 85-23; revised 1985) and the Dutch law on experimental animal care. The university ethical board for animal studies approved all animal experiments reported in this study. The animals used in this study were fed *ad libitum* with food pellets conducted according to the guidelines for Ethics Committee and Animal Experimentation, University of Groningen. The DPBB rat nr 440 (BG 9.9 mM) was fed a hydrolysed casein based diet supplemented with 4% gluten. The other rats were fed a standard cereal based rodent laboratory chow (RmH-B, AB diets, the Netherlands) as described previously[30,31].

Sample preparation. Upon necroscopy, the pancreata were removed, and the tail of the pancreata, most rich in Islets (albeit poor in PP cells), was isolated. Small pieces (~3–5 mm) were cut, followed by immersion fixation in 4% paraformaldehyde (PFA) and 0.1% glutaraldehyde (GA) -that also allows immunostaining- in 0.1 M sodiumcacodylate buffer, pH 7.4 (cacodylate). Alternatively 2% GA and 0.5% PFA was used (datasets 7.2 and 23 mM). Following overnight fixation at 4°C, tissue was embedded in 4% low melting point agarose in 0.1 M cacodylate (~25°C) and directly transferred to ice. The blocks were mounted using acrylate glue. Sixty μm slices were cut from the collected blocks using a HM 650 Micron tissue slicer, fixed for 24 hours in the same fixatives mentioned above, and washed in 0.1 M cacodylate. The Islets of Langerhans and the peripheral acinar parenchyma were selected under a stereomicroscope. Next, Islets were post fixed for two hours in 1% osmiumtetroxide and 1.5% potassium ferrocyanide in 0.1 M cacodylate for 2 hrs at 4°C, rinsed three times for 30 min., dehydrated in a graded series of ethanol and, finally, flat embedded between silane-coated glass slides in epon. Semi-thin (~1 μm) and ultrathin (~60 nm) were cut on an ultramicrotome with a diamond knife (Diatome Inc., Switzerland). The semi-thin sections were stained with 1% toluidine blue (Fig. 1B) or with a mixture of the latter with 0.05% basic fuchsine (Fig. 1C). The ultrathin sections were carefully positioned on single slot M600 Nickel grids (Veco, The Netherlands), to allow acquisition uninterrupted by grid bars. The sections were supported by formvar. Ultrathin sections were stained for 2 min. in 5% uranylacetate in methanol followed by Reynolds lead citrate for another 2 min[32]. Samples were prescreened at low magnification in a transmission electron microscope (CM100; FEI Company, The Netherlands). The best quality samples were selected and subjected to nanotomy. Polysaccharide staining was performed following a modified Thierry protocol[33].

Data acquisition and stitching. All nanotomy data, a total of 25.434 images, were collected on a FEI Tecnai Spirit BioTWIN microscope equipped with LaB$_6$ filament, employing inhouse developed software tools. Samples were extensively pre-irradiated at low magnification prior to data collection to induce sample stabilization by sublimation. The virtual slides for rat412 (DR), rat378, (BG 6.6 mM), rat375 (BG 7.2 mM), rat440 (BG 9.9 mM), rat172 (BG 12 mM), rat367 (BG 23 mM) and rat131 (BG > 30 mM) were recorded at a magnification at the detector plane of 9460× (pixelsize 3.2 nm). Hardware binned 2 k × 2 k images were collected with a FEI Eagle CCD camera: the number of images and the required time is listed in Table 1. Every 10th image, the FEI autofocus routine was employed to maintain the sample at −1 μm defocus.

Data annotation. Annotation has been performed manually. We note that the colour-coding is an indication of the cell type, and might not be 100% accurate. Additional methods such as labelling should be applied in order to define all cell types unambiguously, as discussed in the main text. Atlases and text books[34–38] have been a major source to define cell types based on morphology.

1. Danaei, G. *et al.* National, regional, and global trends in fasting plasma glucose and diabetes prevalence since 1980: systematic analysis of health examination surveys and epidemiological studies with 370 country-years and 2.7 million participants. *Lancet* **378**, 31–40 (2011).
2. van Belle, T. L., Coppieters, K. T. & von Herrath, M. G. Type 1 diabetes: etiology, immunology, and therapeutic strategies. *Physiol Rev* **91**, 79–118 (2011).
3. Pisania, A. *et al.* Quantitative analysis of cell composition and purity of human pancreatic islet preparations. *Lab Invest* **90**, 1661–1675 (2010).
4. Westermark, G. T., Westermark, P., Berne, C. & Korsgren, O. Widespread amyloid deposition in transplanted human pancreatic islets. *N Engl J Med* **359**, 977–979 (2008).
5. Zhou, Q., Brown, J., Kanarek, A., Rajagopal, J. & Melton, D. A. In vivo reprogramming of adult pancreatic exocrine cells to beta-cells. *Nature* **455**, 627–632 (2008).
6. Gray, H. in *Anatomy Descriptive and Surgical* (ed John W. Parker and Son) (1858).
7. Langerhans, P. *Beiträge zur mikroskopischen Anatomie der Bauchspeicheldüse* Med. Dissertation thesis, FRIEDRICH-WILHELMS-UNIVERSITÄT (1869).
8. In't Veld, P. & Marichal, M. Microscopic anatomy of the human islet of Langerhans. *Adv Exp Med Biol* **654**, 1–19 (2010).
9. Faas, F. G. A. *et al.* Virtual nanoscopy: Generation of ultra-large high resolution electron microscopy maps. *The Journal of Cell Biology* **198**, 457–469 (2012).
10. de Lanerolle, P. & Serebryannyy, L. Nuclear actin and myosins: life without filaments. *Nat Cell Biol* **13**, 1282–1288 (2011).
11. Lam-Tse, W. K., Lernmark, A. & Drexhage, H. A. Animal models of endocrine/organ-specific autoimmune diseases: do they really help us to understand human autoimmunity? *Springer Semin Immunopathol* **24**, 297–321 (2002).
12. In't Veld, P. Insulitis in the human endocrine pancreas: Does a viral infection lead to inflammation and beta cell replication? *Diabetologia* **54**, 2220–2222 (2011).
13. Coppieters, K. T. & von Herrath, M. G. Motifs for a deadly encounter. *Nat Immunol* **13**, 205–206 (2012).
14. Eizirik, D. L., Colli, M. L. & Ortis, F. The role of inflammation in insulitis and beta-cell loss in type 1 diabetes. *Nat Rev Endocrinol* **5**, 219–226 (2009).
15. Hanenberg, H., Kolb-Bachofen, V., Kantwerk-Funke, G. & Kolb, H. Macrophage infiltration precedes and is a prerequisite for lymphocytic insulitis in pancreatic islets of pre-diabetic BB rats. *Diabetologia* **32**, 126–134 (1989).
16. Willcox, A., Richardson, S. J., Bone, A. J., Foulis, A. K. & Morgan, N. G. Analysis of islet inflammation in human type 1 diabetes. *Clin Exp Immunol* **155**, 173–181 (2009).
17. Yoon, J. W. & Jun, H. S. Cellular and molecular pathogenic mechanisms of insulin-dependent diabetes mellitus. *Ann N Y Acad Sci* **928**, 200–211 (2001).
18. Coppieters, K., Amirian, N. & von Herrath, M. Intravital imaging of CTLs killing islet cells in diabetic mice. *The Journal of Clinical Investigation* **122**, 119–131 (2011).
19. Virtanen, I. *et al.* Blood vessels of human islets of Langerhans are surrounded by a double basement membrane. *Diabetologia* **51**, 1181–1191 (2008).
20. Jen, J. *et al.* Hereditary endotheliopathy with retinopathy, nephropathy, and stroke (HERNS). *Neurology* **49**, 1322–1330 (1997).
21. Dotta, F. *et al.* Coxsackie B4 virus infection of β cells and natural killer cell insulitis in recent-onset type 1 diabetic patients. *Proceedings of the National Academy of Sciences* **104**, 5115–5120 (2007).
22. Holmberg, R. *et al.* Antiviral treatments reduce severity of diabetes in Ljungan virus-infected CD-1 mice and delay onset in diabetes-prone BB rats. *Microbiol Immunol* **53**, 567–572 (2009).
23. Lacy, P. E. Electron microscopy of the beta cell of the pancreas. *Am J Med* **31**, 851–859 (1961).
24. Toreson, W. E. Glycogen infiltration (so-called hydropic degeneration) in the pancreas in human and experimental diabetes mellitus. *Am J Pathol* **27**, 327–347 (1951).
25. Graf, R. & Klessen, C. Glycogen in pancreatic islets of steroid diabetic rats. Carbohydrate histochemical detection and localization using an immunocytochemical technique. *Histochemistry* **73**, 225–232 (1981).
26. Niklasson, B. Current views on Ljungan virus and its relationship to human diabetes. *J Med Virol* **83**, 1673 (2011).
27. Cardona, A. *et al.* TrakEM2 Software for Neural Circuit Reconstruction. *PLoS One* **7**, e38011 (2012).
28. Phan, S. *et al.* TxBR montage reconstruction for large field electron tomography. *Journal of Structural Biology* **180**, 154–164 (2012).

29. Müller-Reichert, Thomas; Verkade, Paul/Introduction to correlative light and electron microscopy. In: Methods in Cell Biology, Vol. **111**, Muller-Reichert, T. & Verkade, P. (Elsevier, 2012).
30. Visser, J. *et al.* Thymectomy should be the first choice in the protection of diabetes-prone BB rats for breeding purposes. *Lab Anim* **38**, 371–375 (2004).
31. Visser, J. T. *et al.* Restoration of impaired intestinal barrier function by the hydrolysed casein diet contributes to the prevention of type 1 diabetes in the diabetes-prone BioBreeding rat. *Diabetologia* **53**, 2621–2628 (2010).
32. Reynolds, E. S. The use of lead citrate at high pH as an electron-opaque stain in electron microscopy. *J Cell Biol* **17**, 208–212 (1963).
33. Chiappino, M. L., Dawson, C., Schachter, J. & Nichols, B. A. Cytochemical localization of glycogen in Chlamydia trachomatis inclusions. *J Bacteriol* **177**, 5358–5363 (1995).
34. Junqueira, L. C., Carneiro, J. & Long, J. A. *Functional Histology.* fourth edn (Bunge, 1987).
35. Kahn, C. R. *et al. Joslin's Diabetes Mellitus.* 14 edn (Lippincott Williams & Wilkins, 2005).
36. Pavelka, M. & Roth, J. *Functional Ultrastructure.* second edn (Spinger, 2010).
37. Porter, K. R. & Bonneville, M. A. in *Fine Structure of Cells and Tissues* (Lea and Febiger, 1968).
38. Volk, B. W. & Wellman, K. F. *The Diabetic Pancreas.* second edn (Plenum, 1979).

Acknowledgments

Author contributions

Additional information

How to cite this article: Ravelli, R.B.G. *et al.* Destruction of Tissue, Cells and Organelles in Type 1 Diabetic Rats Presented at Macromolecular Resolution. *Sci. Rep.* **3**, 1804; DOI:10.1038/srep01804 (2013).